COMPARISON OF THE HEAT TRANSFER CHARACTERISTICS OF DEVELOPING AND FULLY DEVELOPED FLOW IN SMOOTH TUBES IN THE TRANSITIONAL FLOW REGIME

Everts, M. and Meyer J.P.*
*Author for correspondence
Department of Mechanical and Aeronautical Engineering,
University of Pretoria,
Pretoria, 0002,
South Africa,
E-mail: josua.meyer@up.ac.za

ABSTRACT

The transitional flow regime has been mostly avoided by designers due to uncertainty and perceived chaotic behavior. However, changes in operating conditions, design constraints or additional equipment can cause the flow to operate in the transitional flow regime. Previous work done in the transitional flow regime did not focus specifically on how the heat transfer characteristics change as the flow develops across the tube length. Therefore, the purpose of this study is to investigate and compare the heat transfer characteristics of developing and fully developed flow in the transitional flow regime and is work in progress. An experimental set-up was designed, built and validated and heat transfer measurements were taken at a heat flux of 2 kW/m^2 between Reynolds numbers of 700 and 10 000. The Nusselt numbers varied between 10 and 68, the Prandtl number between 4.9 and 6.8, the Grashof number between 1.89×10^3 and 3.14×10^4 and the Rayleigh number between 9.66×10^3 and 2.24×10^5. It was found that the width of the transitional flow regime decreased along the tube length as the flow approached fully developed flow. Once the flow was fully developed, the width became negligible as the flow fluctuated between the laminar and low-Reynolds-number-end regimes.

INTRODUCTION

Heat exchangers have a wide range of industrial and domestic applications, for example boilers in power plants, air-conditioners in cars and buildings, refrigerators and radiators. Thus engineers need accurate correlations to optimise the design of these heat exchangers in order to ensure efficiency. In the design process they usually have a choice to select between a flow regime that is either laminar or turbulent. As pressure drop is related to pumping power and thus operational running cost, the aim is to obtain high heat transfer coefficients and low pressure drops. Laminar flow provides low pressure drops, but unfortunately low heat transfer coefficients as well, while the opposite is true for turbulent flow. The best compromise between high heat transfer coefficients and low pressure drops might be in the transitional flow regime, between laminar and turbulent flow. Changes in operating conditions, design constraints, additional equipment being installed, equipment being replaced, corrosion and scaling, can also cause that the heat exchangers start to operate in or close to the transitional flow regime.

Designers are usually advised to avoid the transitional flow regime since the flow is believed to be unstable and chaotic and little design information is available.

NOMENCLATURE

A	[m2]	Area
cp	[J/kg.K]	Specific heat at constant pressure
D	[m]	Diameter[1]
EB	[-]	Energy balance
h	[W/m^{2}K]	Heat transfer coefficient
I	[A]	Current
j	[-]	Colburn j-factor
k	[W/mK]	Thermal conductivity
L	[m]	Length
$\dot{m}$	[kg/s]	Mass flow rate
Nu	[-]	Nusselt number
Pr	[-]	Prandtl number
$\dot{Q}$	[W]	Heat input
$\dot{q}$	[W/m^2]	Heat flux
R	[°C/m]	Thermal resistance
Re	[-]	Reynolds number
T	[°C]	Temperature
V	[V]	Voltage
x	[m]	Distance from inlet

Special characters

ρ	[kg/m^3]	Density
μ	[kg/m.s]	Dynamic viscosity

Subscripts

b	Bulk
c	Cross-section
cr	Critical Reynolds number
i	Inlet/ inner
l	Laminar
lre	Low-Reynolds-number-end
m	Mean
o	Outlet/ outer
s	Surface
t	Turbulent

[1] Except when defined differently with a subscript o to indicate outer diameter

In this flow regime the flow alternates between laminar and turbulent and turbulent eddies occur in flashes known as turbulent bursts. This might cause the pressure drop to increase and order of magnitude [1].

Flow regimes have been extensively investigated from as early as 1883, especially focussing on laminar and turbulent flow, while research has been devoted to transitional flow since the 1990s. According to a recent review paper by Meyer [1], flow in the transitional flow regime has been mainly investigated by Professor Ghajar from Oklahoma State University and his co-workers and Professor Meyer from the University of Pretoria and his co-workers. Ghajar and co-workers used local temperature and pressure measurements along a tube length to investigate the effect of different inlet geometries and heating on the heat transfer coefficients and friction factors [2-11] A constant heat flux boundary condition and different mixtures of distilled water and ethylene glycol were used, which resulted in very high Prandtl numbers (up to 160). Furthermore, due to the combined effects of the relatively large tube diameter (15.8 mm), secondary flow effects and high Prandtl numbers, the Rayleigh numbers (product of Grashof number and Prandtl number) were in the order of 10^5 to 10^6 [5]. The Rayleigh number plays an important role in mixed convection heat transfer and is not only used in their flow regime map (to determine whether the flow is dominated by forced or mixed convection) [5], but also in their correlations to predict the Nusselt numbers in the laminar and transitional flow regimes [4].

Meyer and co-workers used a constant surface temperature boundary condition and water as the test fluid, which resulted in significantly lower Prandtl numbers (approximately 7). The fluid was also being cooled and not heated as in studies using a constant heat flux boundary condition. Furthermore, as they considered the average measurements across a tube length, their data contained both developing (laminar and transitional flow regimes) and fully developed (turbulent flow regime) data [12-15]. From literature it is clear that Ghajar and co-workers broke the ground with investigating the effect of inlet geometry and heating on transition, making it possible for others, such as Meyer and co-workers, to follow. This paper is therefore an extension of the work of Ghajar and co-workers and a different Prandtl number range and tube diameter is used. Furthermore, the focus of previous studies was not on the characteristics of developing flow, but rather on the effect of different inlet geometries and enhanced tubes. Up to now, no experimental studies have been specifically devoted to the heat transfer characteristics of developing flow in the transitional flow regime, how it changes along the tube length, and how it differs from that of fully developed flow. Therefore, in order to gain a better understanding of the characteristics of developing flow, the purpose of this study was to experimentally investigate and compare the heat transfer characteristics of developing and fully developed flow of low Prandtl number fluids in a smooth horizontal tube with a relatively small diameter.

EXPERIMENTAL SET-UP

The experimental set-up is shown in Figure 1 and consisted of a closed water loop which circulated the test fluid from a storage tank through a test section and back using two magnetic gear pumps. Water was used as the test fluid and the temperature of the storage tank was kept at 20 ºC using a thermostat bath. As flow pulsations were introduced into the system due to the pump, an accumulator was installed prior to the flow meters to dampen the pulsations. This ensured a constant pressure at the inlet of the test section.

A bypass valve was inserted between the accumulator and the flow meters to allow the water to flow back into the tank. The bypass valve was also used to increase the pump speed for a specific flow rate, since the pulsations decreased with increasing pump speed. The valve positions were continually adjusted to minimise the flow pulsations for all the measurements, since the stability of flow is crucial when studying transitional flow.

Three Coriolis mass flow meters with different capacities (108 *l*/h, 330 *l*/h and 2 180 *l*/h) were installed in parallel to measure the mass flow rates. The mass flow meters had an accuracy of 0.05% and were used according to the flow rate requirements, in order to minimise the uncertainty of the mass flow measurements. After the mass flow meters, the fluid flowed through the calming section to the test section and mixing section and back into the storage tank.

The mass flow rates were controlled by frequency drives that were connected to the pumps, therefore the required flow rate was obtained by increasing or decreasing the pump speed. The frequency drives were also connected to a personal computer via a data acquisition system. A Labview program was used to record the data points and a MATLAB program was used to read the measured raw data and process the results.

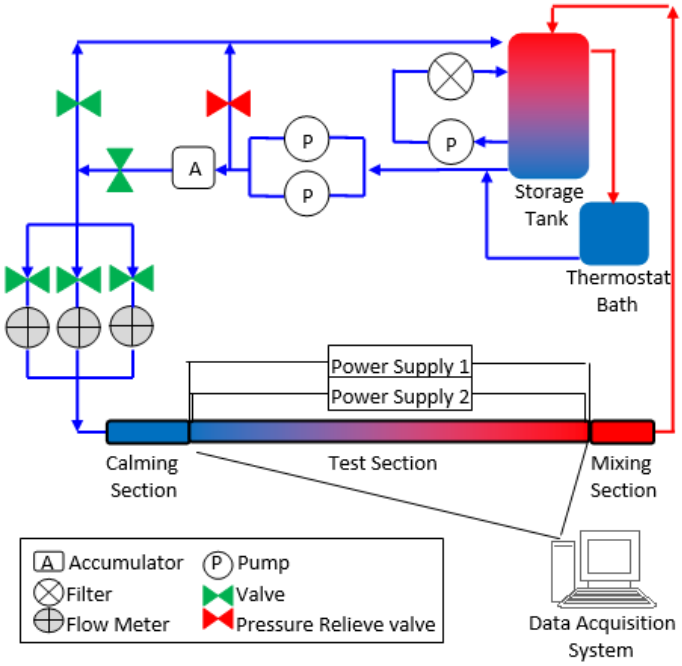

Figure 1 Schematic of experimental set-up used to conduct heat transfer measurements.

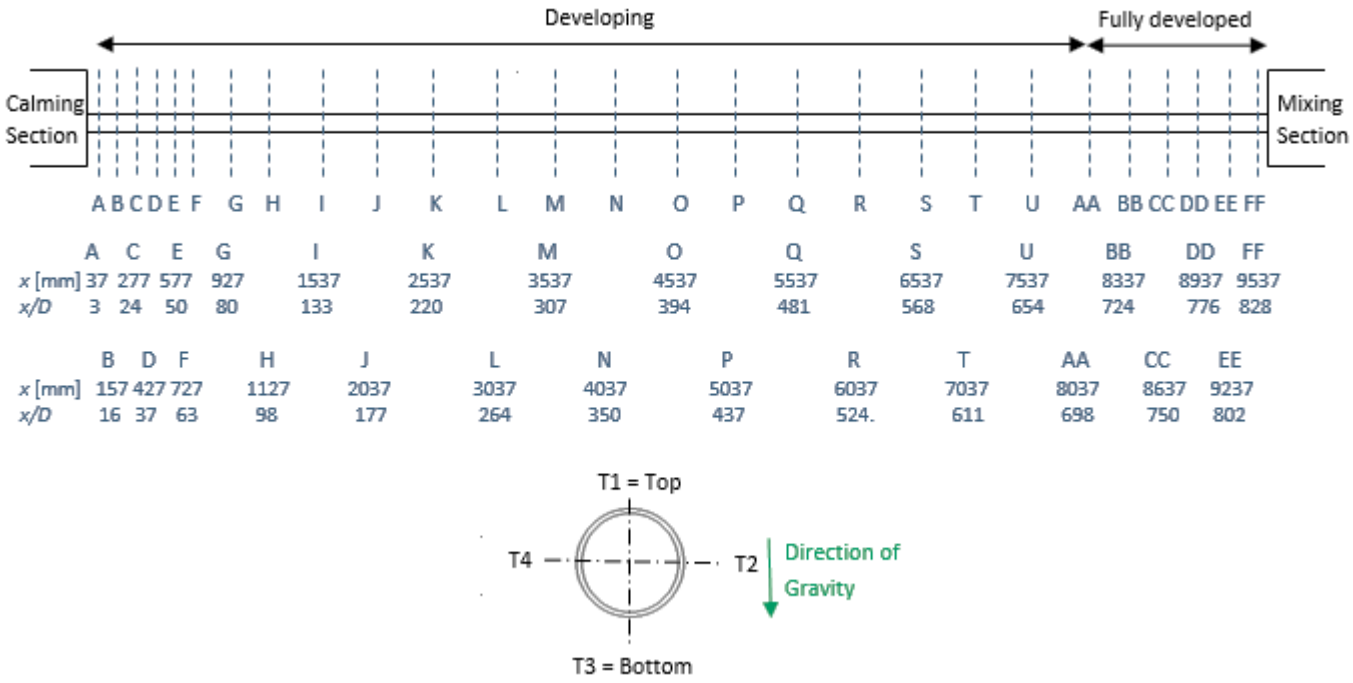

Figure 2 Schematic representation of the test section indicating 21 developing flow thermocouple stations, A-U, and 6 fully developed flow thermocouple stations, AA-FF. A cross-sectional view of the test section is also included to indicate the four thermocouples (T1 to T4) spaced around the periphery of the tube.

A square-edged inlet was used in this study and is characterised by a sudden contraction from the calming section diameter to the test section diameter. The test section was manufactured from a hard-drawn copper tube with an inside and outside diameter of 11.52 mm and 12.7 mm, respectively. The total length of the copper tube was 9.8 m, however temperature measurements were only taken across 9.5 m. In order to prevent any upstream effects from influencing the measurements at the last thermocouple station, 0.3 m was allowed between the last thermocouple station (at x = 9.5 m) and the mixer (at x = 9.8 m). The test section was divided into a developing flow section and a fully developed flow section. The theoretical thermal entrance length ($L_t = 0.05RePrD$) for laminar flow at a Reynolds number of 2 300 and Prandtl number of 6 was calculated to be 7.95 m. Therefore, the first 8 m of the test section was devoted to developing flow, and the remaining 1.5 m to fully developed flow. The total length of the test section provided a maximum length-to-inside diameter ratio (x/D) of 828, while previous studies by Ghajar and co-workers [2-4, 6, 7, 9, 10] and Meyer and Olivier [12] had maximum values of approximately 400 and 350, respectively.

The tube roughness was measured to be approximately 0.455 µm to 0.508 µm, which results in a relative roughness of approximately 0.00004. For all practical purposes, the tube could therefore be considered as a smooth tube.

The test section was insulated with 120 mm thick insulation with a thermal conductivity of 0.034 W/m.K and the maximum theoretical heat loss was calculated to be 2.6%. In order to reduce the theoretical heat loss to less than 2%, the insulation thickness had to be increased to 310 mm, which is an increase of 260%. As recent work on heat transfer in the transitional flow regime [10] reported heat balance errors of ±10%, it was decided that a maximum theoretical heat loss of 2.6% is acceptable.

T-type copper-constantan thermocouples were used to measure the surface temperatures at 27 thermocouple stations along the test section, as shown in Figure 2. Four thermocouples were used at each thermocouple station to investigate possible circumferential temperature distributions caused by secondary flow. The inlet water temperature was measured using a Pt100 inside the calming section, while the outlet water temperature was measured using a Pt100 inside the mixing section. The purpose of the mixing section was to ensure a uniform outlet temperature and the mixer design was based on the work done by Bakker *et al*. [16].

The thermocouples were soldered to the test section by first drilling 1.8 mm depressions into the tube. Flux and solder were inserted into the depression and heated up to the melting point. The thermocouple was then inserted into the depression and the heat was removed in order for the tube to cool down. The thermocouples were checked to ensure good contact with the tube. In-situ calibration was done after the test section was built completely since the properties of the thermocouple junction may change when soldering it to the tube.

To obtain a constant heat flux boundary condition, four constantan wires with a diameter of 0.38 mm were coiled around the test section. The heating wires were connected in parallel to decrease the resistance and current flowing through each wire, in comparison to using a single wire.

DATA REDUCTION

As a constant heat flux boundary condition was applied to the test section, the average axial temperature of the water increased linearly. The bulk fluid temperature was the average of the inlet (obtained from the Pt100 inside the calming section) and outlet (obtained from the Pt100 inside the mixing section) temperatures of the fluid:

$$T_b = \frac{T_{in} + T_{out}}{2} \tag{1}$$

The mean fluid temperature, $T_m(x)$ was the average temperature of the water at a thermocouple station and was found by using the gradient of the line joining the inlet and outlet temperatures of the fluid:

$$T_m(x) = \left(\frac{T_{out} - T_{in}}{L}\right)x + T_{in} \tag{2}$$

The properties of water were determined using the thermophysical correlations for liquid water [17] at the bulk fluid temperature for the average properties and at the mean fluid temperature for the local properties.

The Reynolds number in the test section was calculated as:

$$Re = \frac{\dot{m}D}{\mu A_c} \tag{3}$$

Where $\dot{m}$ is the measured mass flow rate inside the tube, D is the inner-tube diameter, μ is the dynamic viscosity and A_c is the cross-sectional area of the test section. The fluid properties calculated at the bulk fluid temperature were used for the average Reynolds number and the fluid properties calculated at the mean fluid temperature were used to calculate the local Reynolds number at each thermocouple station.

The cross-sectional area of the test section was calculated as follows:

$$A_c = \frac{\pi}{4}D^2 \tag{4}$$

The heat flux was determined from the following equation:

$$\dot{q} = \frac{\dot{Q}_{water}}{A_s} = \frac{\dot{m}C_p(T_{out} - T_{in}))}{\pi DL} \tag{5}$$

The average surface temperature of the test section was calculated from all the surface temperature measurements on the test section, using the trapezoidal rule:

$$T_w = \frac{1}{L}\int_0^L T_w(x)\,dx \tag{6}$$

The thermal resistance across the tube wall was calculated using the following equation:

$$R_{th} = \frac{ln\left(\frac{D_{out}}{D}\right)}{2\pi Lk} \tag{7}$$

However the resistance was found to be negligible and therefore, it could be assumed that the temperature measurements on the outside of the tube wall are the same on the inside of the tube wall.

The average and local heat transfer coefficients at a point x, measured from the inlet of the test section, were then determined from the following equations, since the heat flux, surface temperature, and bulk fluid temperatures were available:

$$h = \frac{\dot{q}}{(T_w - T_b)} \tag{8}$$

$$h(x) = \frac{\dot{q}}{\left(T_w(x) - T_m(x)\right)} \tag{9}$$

The average of the four temperature measurements on the outer surface at a station was used as the inner-surface temperature at a specific thermocouple station, $T_w(x)$, where the local heat transfer coefficient was determined. Again this assumption is valid because of the very small thermal resistance across the tube wall, as indicated in Equation 7.

Finally, the average and local Nusselt numbers were determined as follows:

$$Nu = \frac{hD}{k} \tag{10}$$

$$Nu(x) = \frac{h(x)D}{k(x)} \tag{11}$$

Where k is the thermal conductivity of the fluid obtained using the thermophysical equations of liquid water at the bulk fluid temperature for the average Nusselt number, and at the mean fluid temperature for the local Nusselt number.

The electrical energy input remained constant, resulting in a constant heat flux. The total power input was obtained by measuring the current and voltage drop. The heat transfer rate to the water ($\dot{Q}_{water} = \dot{m}C_p(T_{out} - T_{in})$) was compared with the electrical power $\left(\dot{Q}_{electric} = VI\right)$ of the power supply by using the following energy balance:

$$EB = \left|\frac{\Delta VI - \dot{m}c_p(T_{out} - T_{in})}{VI}\right| * 100 \tag{12}$$

The average energy balance for all experiments was 2.5%.

The heat transfer results were also investigated in terms of the Colburn j-factor to account for the variation in the Prandtl number, which is a function of c_p, μ and k. It was found that during experiments, the viscosity changed significantly and the Prandtl number varied between 3 and 7. The average and local Colburn j-factors were calculated from:

$$j = \frac{Nu}{RePr^{\frac{1}{3}}} \quad (13)$$

$$j = \frac{Nu\,(x)}{Re(x)\,Pr(x)^{\frac{1}{3}}} \quad (14)$$

UNCERTAINTIES

The method suggested by Dunn [18] was used to calculate the uncertainties of the test section and all the uncertainties were calculated within the 95% confidence interval. The uncertainties of the thermocouples and Pt100's were calculated to be 0.1 ºC and 0.031 ºC, respectively. The Reynolds number uncertainty remained approximately constant at 1% for all Reynolds numbers. The Nusselt number and Colburn *j*-factor uncertainties were approximately 3% in the laminar flow regime, but increased as the Reynolds number was increased due to the decreasing temperature difference between the inlet and outlet of the test section, as well as between the surface and fluid. At the maximum Reynolds number, the Nusselt number and Colburn *j*-factor uncertainties were approximately 9%. Both Nusselt number and Colburn *j*-factor uncertainties were slightly higher (5-10%) during transition due to the temperature fluctuations which occurred inside the tube.

VALIDATION

The correlations which were used for the validation, as well as their ranges and reported accuracies, are summarized in Table 1.

For fully developed flow in a circular smooth tube with a constant heat flux boundary condition, the theoretical Nusselt number should be approximately 4.36 [19]. Although it is very challenging to obtain forced convection conditions in macro tubes, when a heat flux of only 60 W/m^2 was applied, the average fully developed Nusselt number ($50 \leq x/D \leq 828$) at a Reynolds number of 940, was found to be 4.746. Although this was within 8.85% of the theoretical value of 4.36, the local surface temperatures were also checked to ensure that the flow was dominated by forced convection. The average deviation between the temperature measurements of the thermocouples at a station was calculated to be 0.04 °C, which was within the uncertainty of the thermocouples. It could therefore be concluded that secondary flow effects were negligible and that fully developed forced convection measurements were successfully obtained in the laminar flow regime. The local Nusselt numbers were also compared with the correlation of Shah and London [20] and the average deviation was 18.58%. A maximum deviation of 65% was obtained at the inlet, while the deviation was less than 3% between $x/D = 567$ and $x/D = 724$.

The average laminar Nusselt numbers obtained at Reynolds numbers between 600 and 2 000 using a heat flux of 1 kW/m^2, were used to validate the average laminar Nusselt numbers for mixed convection conditions. Ghajar and Tam [2] considered the flow to be dominated by mixed convection when the Nusselt numbers deviated more than 15% from the corresponding forced convection Nusselt numbers. This was regarded as a conservative approach since Metais and Eckert [21] used a deviation of 10%. The average laminar Nusselt numbers varied between 8.8 and 9.1, which was more than 200% greater than the fully developed forced convection Nusselt number of 4.36, which confirmed that the flow was dominated by mixed convection. The results correlated well with the correlation of Morcos and Bergles [22] and the average deviation was 5%.

Table 1 Correlations which were used for the validation, as well as the ranges and reported accuracies

Correlation	Percentage deviation
Shah and London [20] $\frac{Nu+1}{5.364[1+(220\ z^*/\pi)^{-10/9}]^{3/10}} = \left[1+\left(\frac{\pi/(115.2\ z^*)}{\{1+(Pr/0.0207)^{2/3}\}^{1/2}\{1+(220\ z^*/\pi)^{-10/9}\}^{3/5}}\right)^{5/3}\right]^{3/10}$	uncertain
Morcos and Bergles [22] $Nu = \left\{4.36^2+\left[0.145\left(\frac{Gr_f^* Pr_f^{1.35}}{Pw_f^{*0.25}}\right)^{0.265}\right]^2\right\}^{1/2}$ $Pw^* = \frac{kD}{k_w t}$ $3\text{x}10^4 \leq Ra_f \leq 10^6$; $4 \leq Pr \leq 175$; $2 \leq Pw \leq 66$	Not given in [22]
Ghajar and Tam [4] $Nu = 0.023\ Re^{0.8}\ Pr^{0.385}\ (x/D)^{-0.0054}(\mu/\mu_w)^{0.14}$ $3 \leq x/D \leq 192$; $7\,000 \leq Re \leq 49\,000$; $4 \leq Pr \leq 34$; $1.1 \leq \mu/\mu_w \leq 1.7$	-10.3% to +10.5%
Gnielinski [23] $Nu = \frac{(\xi/8)(Re-1000)Pr}{1+12.7\sqrt{(\xi/8)}(Pr^{2/3}-1)}\left[1+\left(\frac{D}{L}\right)^{2/3}\right]\left(\frac{Pr}{Pr_w}\right)^{0.11}$ $\xi = (1.8\log_{10} Re - 1.5)^{-2}$ [24] $3\text{x}10^3 \leq Re \leq 5\text{x}10^6$; $0.5 \leq Pr \leq 2\,000$	±20%

To validate the turbulent Nusselt numbers, the Reynolds number was varied between 4 000 and 10 000 and a heat flux of 3 kW/m^2 was applied. The turbulent Nusselt numbers correlated very well with the correlation of Ghajar and Tam [4] with an average deviation of less than 1%. The data also correlated very well with the equation of Gnielinski [23] and the average deviation was approximately 5%. The turbulent Nusselt numbers were also compared with the experimental data of Meyer *et al.* [25], although the experiments were conducted at different heat fluxes. The average deviation between Reynolds numbers of 4 000 and 8 000 was 6%, while a minimum deviation of 4% was found at a Reynolds number of 4 000 and a maximum deviation of 8% was found at a Reynolds number of 7 800.

RESULTS

The Reynolds number, Nusselt number and Colburn *j*-factors were calculated at each thermocouple station (Figure 2) and compared with each other. The results presented in Figures 3 and 4 therefore represents the local heat transfer results, calculated using the properties evaluated at the local temperatures. A total of 61 tests were conducted which consisted of 61 mass flow rate measurements and 6 649 temperature measurements.

Heat Transfer Characteristics of Developing Flow

Figure 3 contains the Nusselt numbers and Colburn *j*-factors at x/D = 13 to x/D = 654 at a heat flux of 2 kW/m^2. The Reynolds number was varied between 700 and 10 000 to ensure that the whole transitional and low-Reynolds-number-end flow regimes, as well as sufficient parts of the laminar and turbulent flow regimes, were covered. The flow was laminar between Reynolds numbers of 700 and approximately 2 500 (depending on the value of x/D), where the Nusselt numbers (Figure 3a) formed a horizontal line and the Colburn *j*-factors (Figure 3b) a straight diagonal line. From Figure 3 it follows that both Nusselt numbers and Colburn *j*-factors in the laminar flow regime decreased with increasing x/D when x/D was less than 133. The local heat transfer coefficients in the laminar flow regime decreased along the tube length as the flow developed and approached fully developed flow, which explains why the Nusselt numbers and Colburn *j*-factors decreased with increasing x/D.

From Figure 3b it follows that the gradient of the Colburn *j*-factors in the laminar flow regime increased with increasing x/D. This is due to the combined effects of developing flow and secondary flow. Secondary flow exists due to the temperature difference between the fluid near the surface and the fluid outside the thermal boundary layer. Near the inlet of the test section, the thermal boundary layer was very thin and the secondary flow effects were suppressed. As the thermal boundary layer increased along the tube length, there was more "room" for secondary flow and therefore the heat transfer coefficients increased. At a fixed Reynolds number, for example Re = 1 000, the flow is closer to fully developed flow than at a Re = 2 500, thus, it would be expected that the heat transfer coefficients should decrease with increasing x/D. However, Ghajar and co-workers [2, 4, 5] found that secondary flow only became significant when x/D was greater than 70 and it was found that in this study, secondary flow effects became significant after x/D = 80. Therefore, the effect of secondary flow would be greater at Re = 1 000 than at a Re = 2 000, since the thermal boundary layer would be thicker and there is more "room" for secondary flow. This explains why the increase in Colburn *j*-factors with increasing x/D, decreased as the Reynolds number increased.

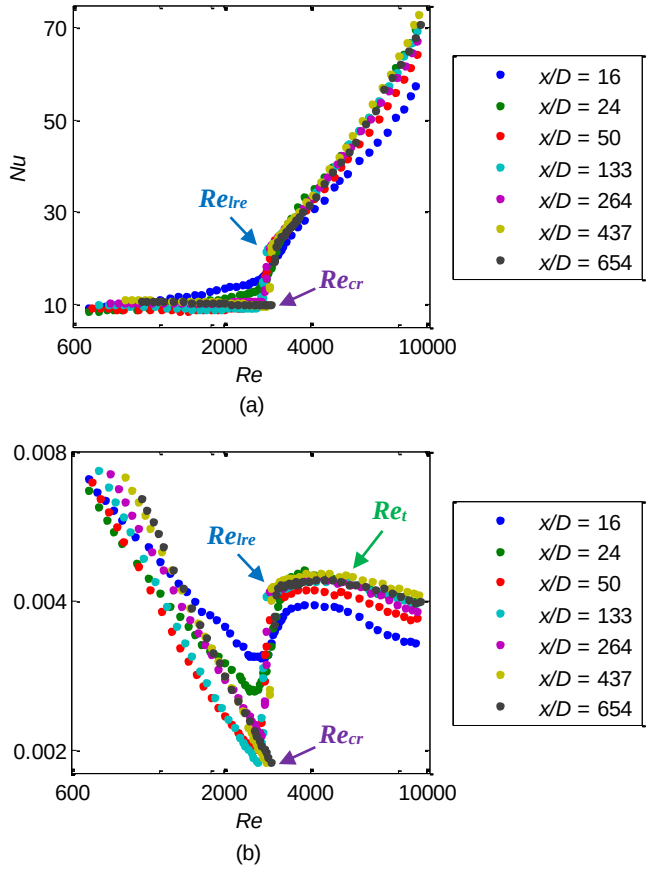

Figure 3 Comparison of local developing (a) Nusselt numbers and (b) Colburn *j*-factors as a function of Reynolds number for x/D = 16 to x/D = 654 at a heat flux of 2 kW/m^2

At a Reynolds number of approximately 2 500 (depending on the value of x/D) both Nusselt numbers and Colburn *j*-factors increased significantly with increasing Reynolds number, which indicates the start of the transitional flow regime (Re_{cr}). From Figure 3b it follows that transition occurred earlier with increasing x/D when x/D was less than 133. However, as x/D was increased further and the flow approached fully developed flow, transition was delayed along the tube length. From both Nusselt numbers and Colburn *j*-factors it follows that the start of transition was very smooth at x/D = 16, but became sharper as the flow developed along the tube length. The end of the transitional flow regime and the start of the low-Reynolds-number-end regime (Re_{lre}) corresponds to the point where the gradient of the Nusselt numbers changed from being almost

vertical (in the transitional flow regime), to diagonal. When the heat transfer coefficients are investigated in terms of the Colburn *j*-factors, it correspond to the point where the gradient of the Colburn *j*-factors began to form a curve after being almost vertical in the transitional flow regime. From both Nusselt numbers and Colburn *j*-factors it follows that the end of the transitional flow regime occurred earlier with increasing *x/D*, thus the width of the transitional flow regime ($Re_{cr} \leq Re \leq Re_{lre}$) decreased as the flow approached fully developed flow.

The end of the low-Reynolds-number-end regime and start of the turbulent flow regime was not clear when the heat transfer coefficients were investigated in terms of Nusselt numbers. However, when the heat transfer coefficients were investigated in terms of the Colburn *j*-factors, the start of the turbulent flow regime (Re_t) corresponded to the point where the gradient of the Colburn *j*-factors changed and became slightly steeper.

Although the Nusselt numbers in Figure 3a continued to increase in the transitional, low-Reynolds-number-end and turbulent flow regimes, a different trend was observed when the heat transfer coefficients were investigated in terms of the Colburn *j*-factor in Figure 3b. This is not unexpected as the Colburn Analogy [19] determined that the relationship between friction factor (pressure drop) and Colburn *j*-factor (heat transfer) is directly proportional. Therefore, the Colburn *j*-factor relationship as a function of Reynolds number, should be similar to that of the friction factor. The product of Prandtl number and Reynolds number ($Pr^{1/3}Re$) increased approximately linearly with increasing Reynolds number, which explains why the Colburn *j*-factors decreased in the laminar, low-Reynolds-number-end and turbulent flow regimes. However, the Nusselt numbers increased significantly in the transitional flow regime ($Re_{cr} \leq Re \leq Re_{lre}$) due to the significant drop in temperature measurements on the surface of the tube. This significant increase led to increasing Colburn *j*-factors in the transitional flow regime.

Heat Transfer Characteristics of Fully Developed Flow

Figure 4 contains the Nusselt number and Colburn *j*-factors at *x/D* = 698 to *x/D* = 802 at a heat flux of 2 kW/m^2. From the laminar Colburn *j*-factors (Figure 4b) it follows that the Colburn *j*-factors at *x/D* was slightly lower between Reynolds numbers of 2 000 and 2 900 than at the other stations and the deviation increased with increasing Reynolds number. This is due to the combined effects of developing flow and secondary flow. At *x/D* = 698, the flow was not yet fully developed, however, it was closer to fully developed flow at *Re* = 2 000 than at *Re* = 2 900. Therefore, as the Reynolds number increased, the thickness of the thermal boundary layer decreased, and thus also the secondary flow effects, which led to decreasing heat transfer coefficients. As *x/D* was increased further, the flow became fully developed and there was no significant change between the laminar Nusselt numbers and Colburn *j*-factors along the remaining part of the tube length.

It would be expected that the Nusselt numbers and Colburn *j*-factors should remain the same along the tube length when the flow is turbulent, since the flow is fully developed. However, Figure 4 it follows that this was not the case. At the maximum Reynolds number, the difference between the Colburn *j*-factors at *x/D* = 724 and *x/D* = 776, was approximately 14%, while the deviation between *x/D* = 724 and *x/D* = 802 was approximately 8%. The maximum Nusselt number and Colburn *j*-factor uncertainty in the turbulent flow regime was approximately 9% due to the very small temperature differences in this flow regime. When one thermocouple station measured slightly higher or lower (although it was still within the uncertainty of the thermocouples), the heat transfer coefficients at that station will be higher or lower than expected. Since the deviation of the turbulent Colburn *j*-factors between *x/D* = 724 and *x/D* = 802 was within the uncertainty of the Colburn *j*-factors, it was considered as insignificant.

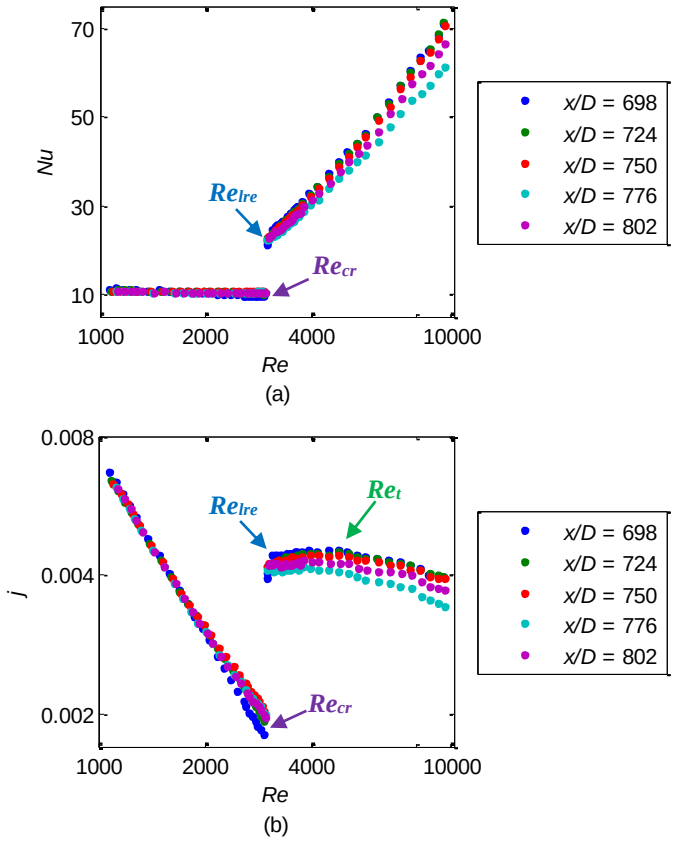

Figure 4 Comparison of local fully developed (a) Nusselt numbers and (b) Colburn *j*-factors as a function of Reynolds number for *x/D* = 698 to *x/D* = 802 at a heat flux of 2 kW/m^2

Transition occurred at a Reynolds number of approximately 2 900 at *x/D* = 698 and was delayed as *x/D* was increased further. However, this delay was not due to developing or fully developed flow. Although transition occurred at the same moment in the entire test section, thus at the same bulk Reynolds number, the local Reynolds numbers increased along the tube length due to the increasing fluid temperature and the variation of fluid properties with temperature. Furthermore, for fully developed flow, the width of the transition region was found to be almost negligible as the flow fluctuated between the laminar flow regime and the low-Reynolds-number-end regime. After time, the flow stabilized as either laminar or in the low-Reynolds-number-end flow regime. For example, at

x/D = 802, the flow stabilised as laminar at Re = 2 956, but at the next Reynolds number (Re = 3 002, an increase of only 1.1%), the flow was in the low-Reynolds-number-end regime.

Although Ghajar and Tam [4] investigated fully developed flow, their transition region was wider than in this study. There are a few possible reasons for this. Different mixtures of ethylene glycol (Prandtl numbers up to 160) were used in their study, therefore the Prandtl number was up to 23 times greater than in this study. Similar calming sections were used, however the diameters of the test sections were different (they used an internal diameter of 15.8 mm). Therefore, the contraction ratio from the calming section to the test section was greater in this study, which might also affect the transition region. Furthermore, as the Grashof number is related to D^3, the Grashof number (and thus buoyancy forces) was at least 2.6 times greater in the study of Ghajar and Tam [4].

The Reynolds number at which the low-Reynolds-number-end regime started also increased with increasing x/D due to the variation of the fluid properties along the tube length. The flow became fully turbulent at a Reynolds number of approximately 4 800, when the Nusselt numbers and Colburn j-factors formed a straight diagonal line.

Transition region of developing and fully developed flow

The Reynolds numbers at which transition started and ended are summarised in Figure 5a. The start of transition occurred at the same moment along the whole tube length, therefore at the same bulk Reynolds number. However, as mentioned earlier, due to the increasing temperature along the tube length and variation of fluid properties with temperature, the local Reynolds number which was calculated at each thermocouple station, increased. The end of transitional flow regime did not occur at the same moment along the tube length and was influenced by the characteristics of developing flow. Between x/D = 13 and x/D = 133, the end of transition occurred earlier along the tube length as the thermal boundary layer developed. Between x/D = 133 and x/D = 698, the flow was not yet fully developed, but transition occurred at approximately the same time along this section of the tube. The increasing Reynolds numbers were thus due to the variation of the fluid temperature. At x/D = 724, the flow became fully developed and transition ended significantly earlier since the flow fluctuated between the laminar and low-Reynolds-number-end flow regimes.

To gain a better understanding of the influence of developing flow on the transition region, the width of the transition region ($\Delta Re = Re_{lre} - Re_{cr}$) as a function of axial position is summarised in Figure 5b. From this graph it follows that the transition region along the tube length can be divided into three sections. Between x/D = 13 and x/D = 169, the width of the transition region decreased along the test section due to development of the thermal boundary layer, and thus the significant increase in thermal boundary layer thickness along the tube length. Temperature fluctuations and secondary flow effects were still fairly limited in this region (secondary flow effects only became significant after x/D = 80) and transition from the laminar to the low-Reynolds-number-end flow regimes occurred gradually. The temperature fluctuations increased along the tube length which led to a decreased transition region between the laminar and low-Reynolds-number-end regimes.

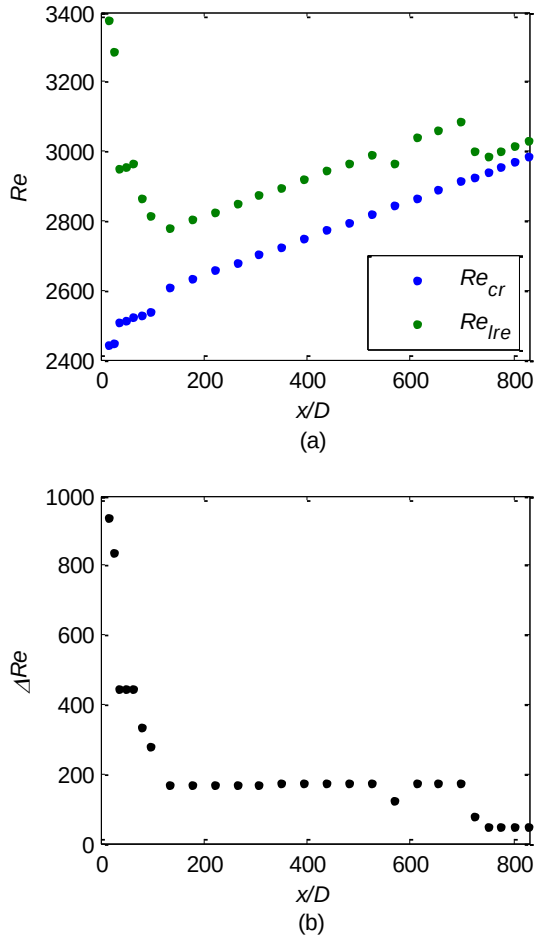

Figure 5 (a) Reynolds numbers at which transition started and ended and (b) width of transition region as a function of axial position at a heat flux of 2 kW/m^2

Between x/D = 169 and x/D = 698, the change in thermal boundary layer thickness as it further developed along the tube length, was almost negligible and transition ended approximately the same time. Secondary flow effects were significant in this region and the temperature fluctuations inside the test section increased along the tube length. This led to a sharper transition from the laminar to low-Reynolds-number-end flow regimes. After x/D = 698, the flow was fully developed. Severe temperature fluctuations occurred inside the test section and the flow alternated between the laminar and low-Reynolds-number-end regions, and the transitional flow regime diminished. Although it seems from Figure 5b as if the width was approximately 46, this was only the increment between the different Reynolds numbers. This increment was the smallest possible change in Reynolds number (or mass flow rate) that could be accommodated in the experimental set-up. Thus, it stabilized as laminar at the one Reynolds number, and then in the low-Reynolds-end-regime at the next Reynolds number.

CONCLUSION

Up to now, no experimental work has been done specifically focussing on how the heat transfer characteristics of developing flow in the transitional flow regime changes along the tube length and how it compares with fully developed flow. The purpose of this study was therefore to experimentally investigate the heat transfer characteristics of developing and fully developed flow in smooth tubes in the transitional flow regime. The Reynolds number was varied between 700 and 10 000 to ensure that the whole transitional and low-Reynolds-number-end regimes, as well as sufficient parts of the laminar and turbulent flow regimes, were covered.

The local Reynolds numbers, Nusselt numbers and Colburn *j*-factors were calculated at each of the 27 thermocouple stations and then compared with each other. The start of transition was smooth near the inlet of the test section, but became sharper as the flow developed along the tube length. Furthermore, the start of transition was not influenced by the characteristics of developing flow and occurred at the same time along the whole tube length. However, the end of transition was influenced by the development of the thermal boundary layer and secondary flow. The transition region across the tube length was divided into three sections. In the first section ($13 \leq x/D \leq 169$), which would be applicable the very short heat exchangers, the transition region decreased along the test section as the thermal boundary layer developed and secondary flow effects became significant. In the second section ($169 \leq x/D \leq 698$), which would be applicable to most heat exchanger applications, the width of the transition region remained constant. Transition ended at approximately the same time and the change in the thermal boundary layer as it developed long the test section was approximately negligible. In the last section, the flow was fully developed and due to the severe temperature fluctuations that occurred inside the test section, the flow fluctuated between the laminar and low-Reynolds-number-end regimes. Therefore, the transitional flow regime diminished once the flow became fully developed. It can therefore be concluded that the heat transfer characteristics of developing and fully flow in the transitional flow regime are significantly different.

ACKNOWLEDGEMENTS

The funding obtained from the NRF, Stellenbosch University/ University of Pretoria Solar Hub, CSIR, EEDSM Hub, RDP and NAC is acknowledged and duly appreciated.

REFERENCES

[1] J. P. Meyer, "Heat transfer in tubes in the transitional flow regime," presented at the 15th International Heat Transfer Conference, Kyoto, Japan, 2014.

[2] A. J. Ghajar and L. M. Tam, "Laminar-transition-turbulent forced and mixed convective heat transfer correlations for pipe flows with different inlet configurations," in *Winter Annual Meeting of the American Society of Mechanical Engineers*, New York, NY, United States Atlanta, GA, USA, 1991, pp. 15-23.

[3] A. J. Ghajar and K. F. Madon, "Pressure drop measurements in the transition region for a circular tube with three different inlet configurations," *Experimental Thermal and Fluid Science*, vol. 5, pp. 129-135, 1992.

[4] A. J. Ghajar and L. M. Tam, "Heat transfer measurements and correlations in the transition region for a circular tube with three different inlet configurations," *Experimental Thermal and Fluid Science*, vol. 8, pp. 79-90, 1994.

[5] A. J. Ghajar and L. M. Tam, "Flow regime map for a horizontal pipe with uniform wall heat flux and three inlet configurations," *Experimental Thermal and Fluid Science*, vol. 10, pp. 287-297, 1995.

[6] L. M. Tam and A. J. Ghajar, "Effect of Inlet Geometry and Heating on the Fully Developed Friction Factor in the Transition Region of a Horizontal Tube," *Experimental Thermal and Fluid Science*, vol. 15, pp. 52-64, 1997.

[7] L. M. Tam and A. J. Ghajar, "The unusual behavior of local heat transfer coefficient in a circular tube with a bell-mouth inlet," *Experimental Thermal and Fluid Science*, vol. 16, pp. 187-194, 1998.

[8] A. J. Ghajar, C. C. Tang, and W. L. Cook, "Experimental investigation of friction factor in the transition region for water flow in minitubes and microtubes," *Heat Transfer Engineering*, vol. 31, pp. 646-657, 2010.

[9] H. K. Tam, L. M. Tam, A. J. Ghajar, S. C. Tam, and T. Zhang, "Experimental investigation of heat transfer, friction factor, and optimal fin geometries for the internally microfin tubes in the transition and turbulent regions," *Journal of Enhanced Heat Transfer*, vol. 19, pp. 457-476, 2012.

[10] H. K. Tam, L. M. Tam, and A. J. Ghajar, "Effect of inlet geometries and heating on the entrance and fully-developed friction factors in the laminar and transition regions of a horizontal tube," *Experimental Thermal and Fluid Science*, vol. 44, pp. 680-696, 2013.

[11] L. M. Tam, H. K. Tam, A. J. Ghajar, W. S. Ng, and C. K. Wu, "The effect of inner surface roughness and heating on friction factor in horizontal mini-tubes," presented at the 15th International Heat Transfer Conference, Kyoto, Japan, 2014.

[12] J. A. Olivier and J. P. Meyer, "Single-phase heat transfer and pressure drop of the cooling of water inside smooth tubes for transitional flow with different inlet geometries (RP-1280)," *HVAC and R Research*, vol. 16, pp. 471-496, 2010.

[13] J. P. Meyer and J. A. Olivier, "Transitional flow inside enhanced tubes for fully developed and developing flow with different types of inlet disturbances: Part II-heat transfer," *International Journal of Heat and Mass Transfer*, vol. 54, pp. 1598-1607, 2011.

[14] J. P. Meyer and J. A. Olivier, "Transitional flow inside enhanced tubes for fully developed and developing flow with different types of inlet disturbances: Part I - Adiabatic pressure drops," *International Journal of Heat and Mass Transfer*, vol. 54, pp. 1587-1597, 2011.

[15] J. P. Meyer and J. A. Olivier, "Heat transfer and pressure drop characteristics of smooth horizontal tubes in the transitional flow regime," *Heat Transfer Engineering*, vol. 35, pp. 1246-1253, 2014.

[16] A. Bakker, R. D. LaRoche, and E. M. Marshall. (2000, 24 February). *Laminar flow in static mixers with helical elements*. Available: http://www.bakker.org/cfmbook/lamstat.pdf

[17] C. O. Popiel and J. Wojtkowiak, "Simple formulas for thermophysical properties of liquid water for heat transfer calculations [from O°C to 150°C," *Heat Transfer Engineering*, vol. 19, pp. 87-101, 1998.

[18] P. F. Dunn, *Measurement and Data Analysis for Engineering and Science*, 2nd ed. United States of America: CRC Press, 2010.

[19] Y. A. Cengel, *Heat and Mass Transfer: A Practical Approach*, 3rd ed. Singapore: McGraw-Hill, 2006.

[20] R. K. Shah and A. L. London, *Laminar Flow Forced Convection in Ducts*. New York: Academic Press, 1978.

[21] B. Metais and E. Eckert, "Forced, mixed, and free convection regimes," *Journal of Heat Transfer*, vol. 86, pp. 295-296, 1964.

[22] S. M. Morcos and A. E. Bergles, "Experimental investigation of combines forced and free laminar convection in horizontal tubes," *Journal of Heat Transfer*, vol. 97, pp. 212-219, 1975.

[23] V. Gnielinski, "New equations for heat and mass-transfer in turbulent pipe and channel flow," *International Chemical Engineering*, vol. 16, pp. 359-368, 1976.

[24] G. K. Filonenko, "Hydraulischer Widerstand von Rohrleitungen (Orig. Russ.)," *Teploenergetika*, vol. 1, pp. 40-44, 1954.

[25] J. P. Meyer, T. J. McKrell, and K. Grote, "The influence of multi-walled carbon nanotubes on single-phase heat transfer and pressure drop characteristics in the transitional flow regime of smooth tubes," *International Journal of Heat and Mass Transfer*, vol. 58, pp. 597-609, 2013.